
This is an electronic reprint of the original article.
This reprint may differ from the original in pagination and typographic detail.

Dotel, Utsav Raj; Davodi, Fatemeh; Sorsa, Olli; Kallio, Tanja; Hemmingsen, Tor
Nitrogen doped Carbon Nanotubes as Electrocatalyst for Oxygen Reduction Reaction

Published in:
International Journal of Electrochemical Science

DOI:
[10.20964/2019.11.06](https://doi.org/10.20964/2019.11.06)

Published: 01/11/2019

Document Version
Publisher's PDF, also known as Version of record

Published under the following license:
CC BY

Please cite the original version:
Dotel, U. R., Davodi, F., Sorsa, O., Kallio, T., & Hemmingsen, T. (2019). Nitrogen doped Carbon Nanotubes as Electrocatalyst for Oxygen Reduction Reaction. *International Journal of Electrochemical Science*, 14(11), 10340-10351. <https://doi.org/10.20964/2019.11.06>

This material is protected by copyright and other intellectual property rights, and duplication or sale of all or part of any of the repository collections is not permitted, except that material may be duplicated by you for your research use or educational purposes in electronic or print form. You must obtain permission for any other use. Electronic or print copies may not be offered, whether for sale or otherwise to anyone who is not an authorised user.

Nitrogen doped Carbon Nanotubes as Electrocatalyst for Oxygen Reduction Reaction

Utsav Raj Dotel¹, Fatemeh Davodi², Olli Sorsa², Tanja Kallio², Tor Hemmingsen^{1,*}

¹ Department of Natural Science and Mathematics, University of Stavanger, NO-4036 Stavanger, Norway

² Department of Chemistry and Material Science, Aalto University, Kemistintie 1 D 1 02150 Espoo, Finland

*E-mail: tor.hemmingsen@uis.no

Received: 25 February 2019 / Accepted: 15 July 2019 / Published: 7 October 2019

The oxygen reduction reaction on nitrogen doped multiwalled carbon nanotubes (N-MCNTs) is studied for its application for deoxygenation of seawater. N-MCNTs were synthesized using commercial MCNTs and polyaniline as nitrogen precursor and annealing at a high temperature. The ORR was studied on N-MCNTs in 0.5 M sodium chloride solution using a rotating disk electrode, and physical characterization of the electrocatalysts was performed using X-ray diffraction, mass spectroscopy and transmission electron microscope techniques. The material showed high activity for the ORR in the chloride electrolyte. The onset potential for N-MCNTs was 0.94 V vs RHE. Koutecky-Levich analysis showed that the electrons transfer mainly followed the four-electron pathway, and the electrocatalyst showed good stability during a 15-h stability test.

Keywords: Seawater, Deoxygenation, Oxygen reduction, Carbon nanotubes.

1. INTRODUCTION

Seawater is injected into the reservoir in order to enhance the oil recovery (EOR). In order to avoid corrosion of the pipelines, it is necessary to reduce the oxygen effectively to low levels. The oxygen might be removed by electrochemical methods, but, due to the slow kinetics of the oxygen reduction reaction (ORR) at neutral pH and slow reaction rates at low temperature, the commercialization of such deoxygenation cells is difficult [1]. This also applies to other electrochemical systems operating under similar conditions, *e.g.* microbial fuel cells [2-3]. Such deoxygenation cells for seawater have already been investigated on an industrial scale for EOR purposes [4].

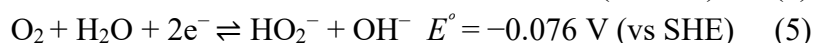
The ORR can proceed in acidic or alkaline solutions, either *via* four- (see Equations (1) or (4)) or alternatively *via* two-electron transfer pathways (Equations (2) and (3) or Equations (5) and (6)). The

exact mechanism depends both on the media and the catalyst used for enhancing this reaction. Of these, the direct four-electron reduction is the desirable pathway for deoxygenation systems, since the ORR following the two-electron transfer pathway forms hydrogen peroxide or peroxide ions, shown in Equations (2) and (5). This may increase the corrosion of the pipes and also damage the cathode material in the cell [5].

In general, the ORR can proceed in acidic media *via* the following pathways:



And in alkaline/neutral media *via*:



Due to the industrial importance of the ORR, extensive studies have been carried out on carbon-based catalysts, metal-based catalysts, metal-carbon hybrids, metal-nitrogen-carbon complexes and biocatalysts, for the development of efficient and durable electrocatalysts for the ORR; see review by Yuan et al. [6]. Platinum and platinum-based materials promote the reaction very efficiently, and the ORR has relatively low overpotentials on such electrocatalysts [7-8]. However, platinum-based materials do not fulfill sustainability criteria because of their high price and scarcity [9]. In addition, their catalytic activity decreases drastically, due to interactions with anions under “polluted” environmental conditions [10-14]. Alternative materials have been developed, such as non-Pt catalysts in alkaline [15-16] and acidic [8] media for the ORR. In a neutral aqueous chloride solution, there are, however, only a few studies on oxygen reduction catalysts. For a seawater system using deoxygenation cells, the study of the reduction reactions of oxygen in a chloride containing electrolyte is essential. Silver-plated brass and silver-plated Monel have been tested for the removal of oxygen from seawater, but the kinetics for oxygen reduction on silver are quite slow [17-22] compared to platinum in other electrolytes [23-24]. In addition, galvanic corrosion might occur and result in erosion of the electroplated silver [4].

This study presents the utilization of nitrogen doped multiwalled carbon nanotubes (N-MCNT) as a novel alternative for the reduction of oxygen in an aqueous chloride electrolyte. The large surface area and high corrosion resistance of carbon nanotubes make them a suitable candidate for a catalyst for seawater deoxygenation applications. N-MCNTs were synthesized using the recently introduced facile method for controlling the nitrogen moiety type [25]. N-MCNTs show a higher onset potential with satisfactory durability for seawater deoxygenation, compared to commercially available catalysts.

2. EXPERIMENT

2.1. Preparation of N-MCNTs

The procedure for the N-MCNT synthesis is reported by Davodi et al [25]. Briefly, 40 mg multiwalled CNTs (Nanocycle) were dispersed in a diluted HCl solution and stirred for 5 minutes, and

100 mg fresh polyaniline powder was dispersed in a diluted HCl solution. Subsequently, both solutions were mixed together, and the final product was separated and annealed for 1 h at 800 °C under a nitrogen atmosphere.

2.2. Physical characterization

The N-MCNTs were analyzed by high resolution transmission electron microscopy (HRTEM) (JEM 2100). X-ray photoelectron spectroscopy (XPS) was utilized for studying active nitrogen species on N-MCNTs. X-ray diffraction (XRD) studies were performed for N-MCNTs by Panalytical X'pert Pro at room temperature, with the samples placed on a glassy carbon electrode used for electrochemical measurement.

Quantitative analyses of the iron content in N-MCNTs were performed by inductively coupled plasma mass spectrometry (ICP-MS) (NexION 300X, Perkin Elmer). Four samples of N-MCNTs were weighed, and the carbon was fully oxidized at 500 °C for 12 h. The resultant Fe oxides were dissolved in boiling HCl (30%, Suprapure®, Merck) for 3 h. After dilution of the acid to 50 ml, the samples were introduced into the ICP-MS. Two blank crucibles underwent the same procedure, to account for experimental Fe contamination.

2.3. Electrochemical characterization

Cyclic voltammetry (CV) and linear sweep voltammetry (LSV) analyses were performed for N-MCNTs, using a rotating disk electrode (RDE) set-up (Pine Instrument Company, USA) and a potentiostat (Metrohm Autolab). The electrolyte, 0.5 M NaCl solution, was prepared from reagent grade NaCl (Sigma-Aldrich) in millipore water (18.2 MΩ cm). A glassy carbon disc ($D = 5$ mm, $A = 0.196$ cm²), a reversible hydrogen electrode (RHE) and a platinum wire were used as the working, reference and counter electrode, respectively. The glassy carbon surface was polished using 5 μm, 0.3 μm and 0.05 μm alumina slurries to give a mirror finish. The glassy carbon had the total catalyst loading of 40 μg N-MCNT, and 5 μL of 0.05 wt.% Nafion solution (Sigma-Aldrich) was applied to the top of the catalyst layer.

Before each CV and LSV test, nitrogen (5.0 grade, AGA) or oxygen (5.0 grade, AGA) was purged into the solution, in order to perform experiments in both nitrogen-saturated and oxygen-saturated environments. The scan rate for CV was 50 mV s⁻¹ in the potential range of 0 to 1.1 V vs RHE. LSV was performed in the potential range of 1.2 to 0 V vs RHE at the scan rate of 10 mV s⁻¹ at 0, 400, 700, 1200, 1600, 2000 and 2500 rpm.

Durability tests were performed with N-MCNT cycling 1600 times (corresponding to 15 h) in an oxygen-saturated 0.1 M NaOH solution because the cathodic section of a deoxygenation cell becomes alkaline [3], and a higher pH has an impact on the stability of the cathode material. The linear sweep voltammograms were performed before and after the cycling at 1600 rpm.

3. RESULTS AND DISCUSSION

The morphology of N-MCNTs has been investigated by HRTEM (Figure 1). The average diameter of N-MCNTs is measured to be approximately 10 nm. As shown in Figure 1, the quality of the nanotubes is preserved during the synthesis, and the graphite structure of the nanotubes is intact after nitrogen doping. It has been demonstrated that nitrogen dopant on the surface of carbon material is essential, to obtain metal-free ORR electrocatalysts [26], and the observed catalytic activity on N-MCNT has been attributed to pyridinic and graphitic-type nitrogen groups; see Figure 2 [27-29].

The elemental composition and different surface structural groups of nitrogen in N-MCNTs are determined using XPS, as shown in Figure 3. Results from the XPS analyses of N-MCNTs showed ~1.3 at.% nitrogen content. The N1s spectra of the pyrolyzed N-MCNT material is deconvoluted to the three main peaks. The peaks at 398.4 and 400.7 eV are attributed to the pyridinic and graphitic nitrogen, respectively. The third peak at 402.6 eV corresponds to the protonized imine nitrogen [25]. Using this data, the shares of the different nitrogen moieties in N-MCNT are as follows: 45 at.% of pyridinic nitrogen, 45 at.% quaternary nitrogen and 10 at.% protonized imine nitrogen.

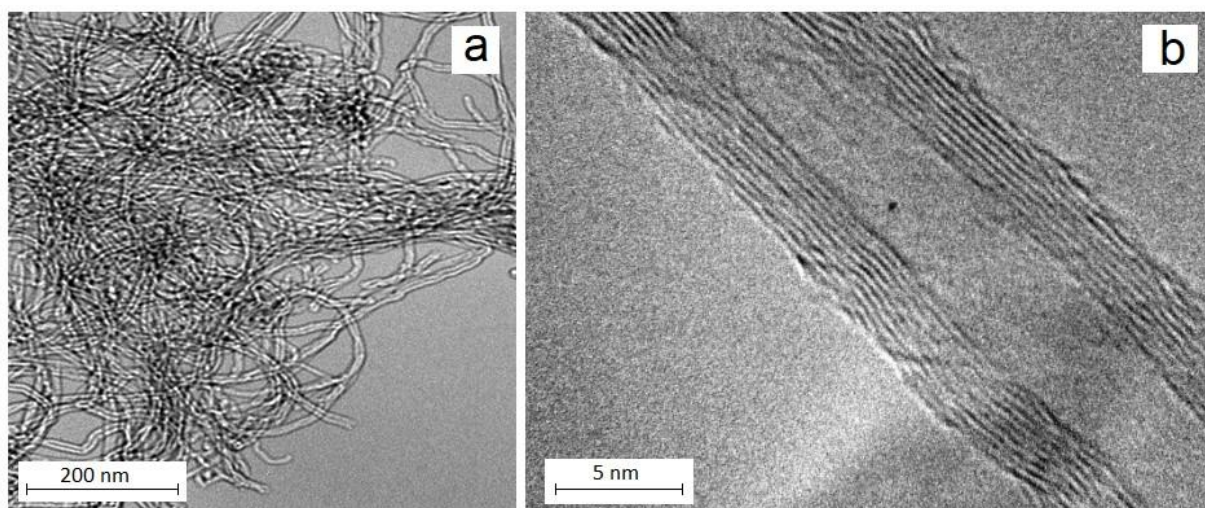


Figure 1. HRTEM images of N-MCNTs.

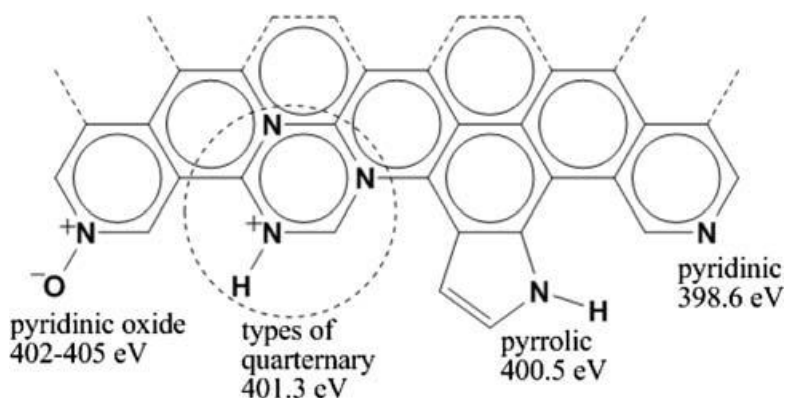


Figure 2. N-CNT structures [29].

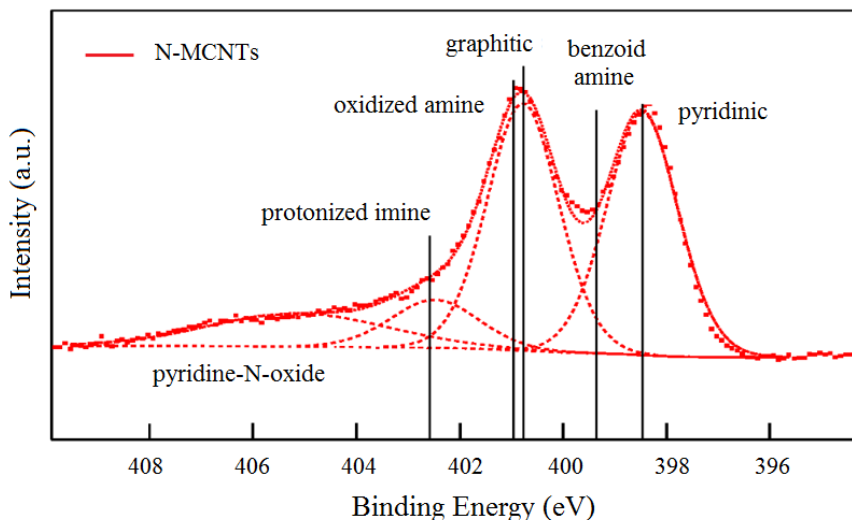


Figure 3. XPS spectrum of N-MCNTs after pyrolysis.

Furthermore, N-MCNTs have been investigated by XRD, as shown in Figure 4. Two smaller crystalline peaks were observed for N-MCNTs at 31.5° and 37° , indicating the small amounts of iron oxide (magnetite). According to ICP-MS measurements, N-MCNTs contain 0.12 wt.% of iron.

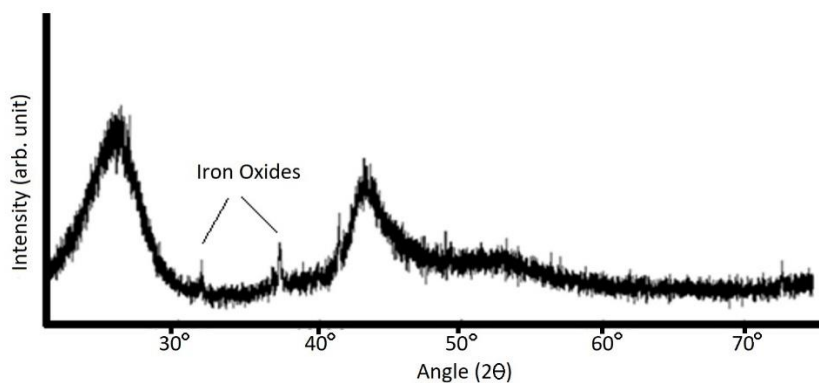


Figure 4. The XRD diffractograms of the N-MCNT.

A rotating glassy disk electrode covered with N-MCNTs was exposed to a 0.1 M NaOH, a 0.5 M H_2SO_4 or a 0.5 M NaCl electrolyte, which was swept between a potential of 1.2V and 0 V. The increase in rotation rate results, as expected, in an increase in the limiting current densities for the ORR, indicating a mass transport limited reaction; see Figure 5. The rate-determining step in ORR is a pH-independent process [19], while the overall ORR process is dependent on pH [30]. The onset potentials for the oxygen reduction in LSV for N-MCNT in 0.5 M NaCl is 0.94 V vs RHE, indicating that N-MCNTs show higher oxygen reduction activity. The onset potentials for ORR in 0.1 M NaOH and 0.5 M H_2SO_4 were analyzed to be 0.89 V and 0.63 V vs RHE, respectively. From Figure 5, the observed limiting current densities for N-MCNTs at 0.2 V vs RHE at 1600 rpm are 4.4 mA cm^{-2} (in 0.5 M NaCl)

and 5 mA cm^{-2} (in 0.1 M NaOH), while they have not reached limiting current yet in acidic media. N-MCNTs reached mass-transfer limited region at about 0.8 V in 0.5 M NaCl at 1600 rpm with a current density of approx. 4.0 mA cm^{-2} ; however, a clear plateau is not observed. This kind of behavior is typical for a carbon catalyst [31-32]. $E_{1/2}$ for N-MCNT in 0.5 M NaCl is observed at 0.86 V vs RHE at 1600 rpm , and the current density is 2.03 mA cm^{-2} . The LSV for N-MCNT at 1600 rpm in acidic, alkaline and neutral solutions is compared with LSV for $20\% \text{ Pt/C}$ in 0.1 M NaOH solution in Figure 5c. The onset potential and ORR activity for $20\% \text{ Pt/C}$ is higher in 0.1 M NaOH compared to neutral and acidic media; thus, it is used as a reference. $20\% \text{ Pt/C}$ was not tested in 0.5 M NaCl because the strong adsorption bond strength of Cl^- on Pt causes Cl^- adsorption, forming Pt-Cl complex, whose reduction overlaps with the oxygen reduction curve, making the analysis difficult [33]. The onset potential for ORR for $20\% \text{ Pt/C}$ in 0.1 M NaOH is close to onset potential for N-MCNT in 0.5 M NaCl . Unlike carbon nanotubes, a clear plateau is observed on Pt/C, with a limiting current density of approx. 6 mA/cm^2 . Artyushkova et al. reported that the ORR electrochemical activity of platinum group metal (PGM) free catalysts is affected by the electrolytes' pH, with the change in the concentration of protons and hydroxyls in an electrolyte leading to changes in the surface chemistry of the catalyst, and neutral pH is found to have higher electrochemical activity [34]. The pH affects the chemical state and the accessibility of active sites (moieties) by molecular oxygen.

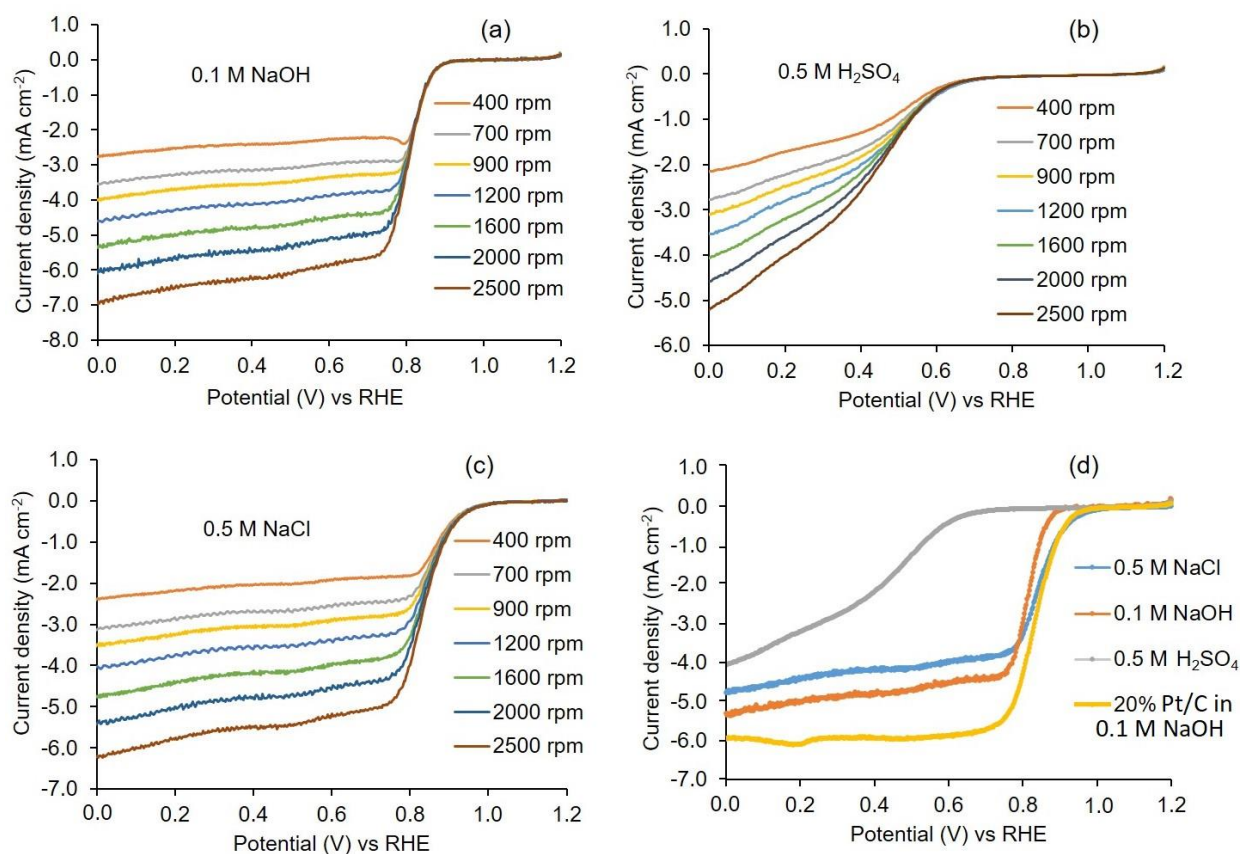


Figure 5. RDE voltammogram for the ORR on N-MCNT in (a) 0.1 M NaOH , (b) $0.5 \text{ M H}_2\text{SO}_4$, and (c) 0.5 M NaCl . (d) Comparison of RDE voltammogram between N-MCNT (in acidic, alkaline and neutral media) and $20\% \text{ Pt/C}$ in alkaline media.

The results obtained for N-MCNT in acidic, neutral and alkaline media are compared with results for commercially available catalysts. Limited work has been accomplished on chloride solution; thus, for reference, the results are compared with ORR in alkaline media in Table 1.

Table 1. Comparison of catalysts for oxygen reduction reaction [15].

Catalyst	Onset Potential vs RHE (V)*	Tafel slope (mV dec ⁻¹)*
20% Pt/C	1.07	-57
	0.91	-120
Pd/C	0.97	-60
	0.86	-125
20% Ag/C	1.02	-
	0.87	-
Ag (110)	0.91	-80
	0.70	-123
Ag (111)	0.88	-85
	0.64	-125
N-MCNTs	0.77	-
	0.59	-
Ag-CNT	0.85	-
	0.74	-
N-MCNTs (this work)	0.89*	-68*
N-MCNTs (this work)	0.94**	-107**
N-MCNTs (this work)	0.63***	-123***

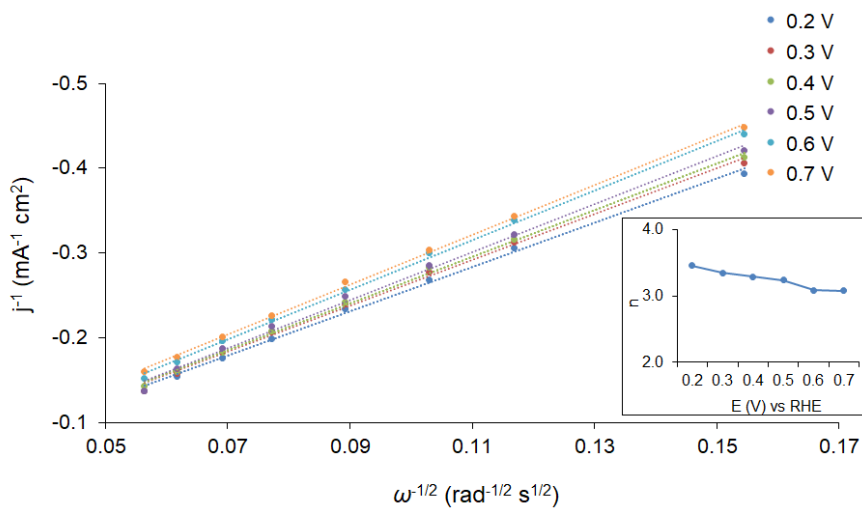
*0.1 M NaOH; **0.5 NaCl; ***0.5 M H₂SO₄

The data obtained from the RDE measurements at different rotation rates for N-MCNT have been analyzed using the Koutecky-Levich (K-L) method; see Equation (7) [35].

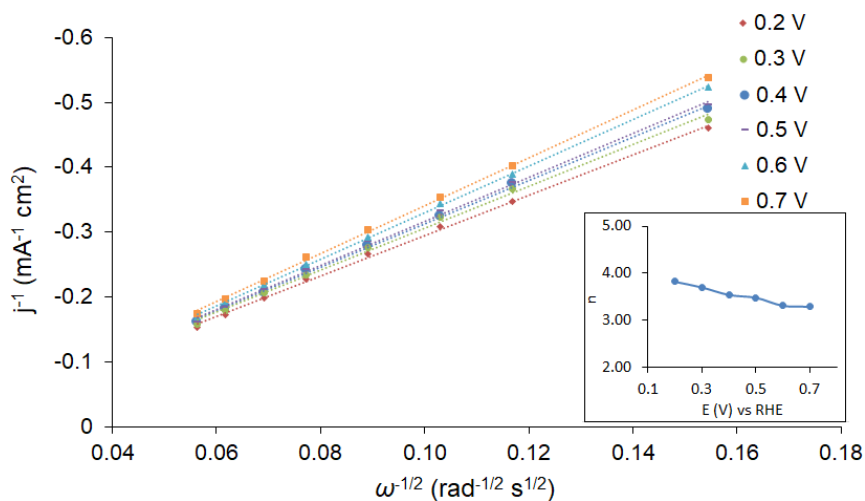
$$\frac{1}{j} = \frac{1}{j_k} + \frac{1}{j_d} = \frac{1}{j_k} + \frac{1}{B\omega^{1/2}} \quad (7)$$

where j is the measured limiting current density; j_k and j_d are the kinetic and diffusion limited current densities, respectively; $j_k = nFkC_O$ and $j_d = B\omega^{1/2}$ and B is the Levich slope, which is equal to $0.62nFD_O^{2/3}\nu^{-1/6}C_O$; n is the number of electrons; F is the Faraday constant (96485 C/mol); k is the rate constant for oxygen reduction; D_O is the diffusion coefficient of oxygen in 0.5 M NaCl solution ($1.46 \times 10^{-5} \text{ cm}^2 \text{ s}^{-1}$) [36]; C_O is the bulk concentration of oxygen in 0.5 M NaCl solution ($1 \times 10^{-6} \text{ mol cm}^{-3}$) [37]; ν is the kinematic viscosity of the solution ($0.01 \text{ cm}^2/\text{s}$); and ω is the electrode rotation rate (rad s^{-1}). Note that the viscosity, concentration and diffusion coefficients are different in different electrolytes. The K-L plots for different potentials, 0.7, 0.6, 0.5, 0.4, 0.3 and 0.2 V vs RHE, for N-MCNT in 0.5 M NaCl, are displayed in Figure 6. The number of electron transfer 'n', was calculated using the equation $j_d = 0.62nFD_O^{2/3}\nu^{-1/6}C_O$. The number of electron transfer is measured to increase from 3.3 to 3.8 in 0.5 M NaCl at the potential range of 0.7 V to 0.2 V vs RHE, suggesting that the ORR proceeds with mixed kinetics *via* two- and four-electron transfer pathways at higher potential, and solely approaches the latter

at lower potentials. The number of electron transfer in 0.5 M H₂SO₄ is measured around 2.3 at the potential range of 0.4 V to 0.2 V vs RHE, suggesting the reduction of oxygen by mostly following a two-electron pathway, which is in agreement with investigations by Alexeyeva et al. [38] and Wang et al. [39] In 0.1 M NaOH, the ORR follows similar kinetics to neutral solution, *via* two- and four-electron transfer pathways at higher potential and close to four-electron transfer at lower potential. Similar mechanisms and results in alkaline media are reported for MCNT in the literature [40]. The results indicate that N-MCNT is a suitable catalyst for oxygen reduction in the aqueous chloride solution and is a good choice for a deoxygenation cell.



(a)



(b)

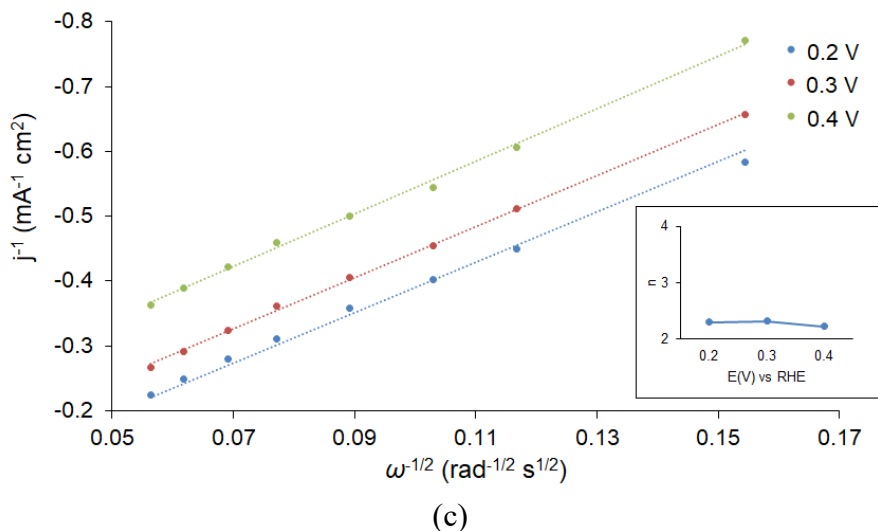


Figure 6. K-L plot for N-MCNT in (a) 0.5 M NaOH, (b) 0.5 M NaCl, and (c) 0.5 M H₂SO₄.

Information regarding the mechanism of O₂ reduction on N-MCNTs can be obtained through the Tafel slopes obtained from the LSV data (Figure 7). The Tafel slope (after *iR* corrections) is measured to be about -107 mV dec^{-1} for N-MCNT in 0.5 M NaCl solution. The Tafel slope for N-MCNT in 0.1 M NaOH is measured to be -69 mV dec^{-1} , and in 0.5 M H₂SO₄ is measured to be -123 mV dec^{-1} . The lowest Tafel plot showed that the ORR activity for N-MCNT is highest in an alkaline media, followed by a neutral media.

The stability of the studied catalyst has been examined by performing 1600 CV cycles over 15 h in the oxygen-saturated 0.1 M NaOH solution, as, during the oxygen removal, the electrode potential will increase from the neutral pH. In Figure 8, the RDE voltammograms at 1600 rpm are compared before and after the stability test.

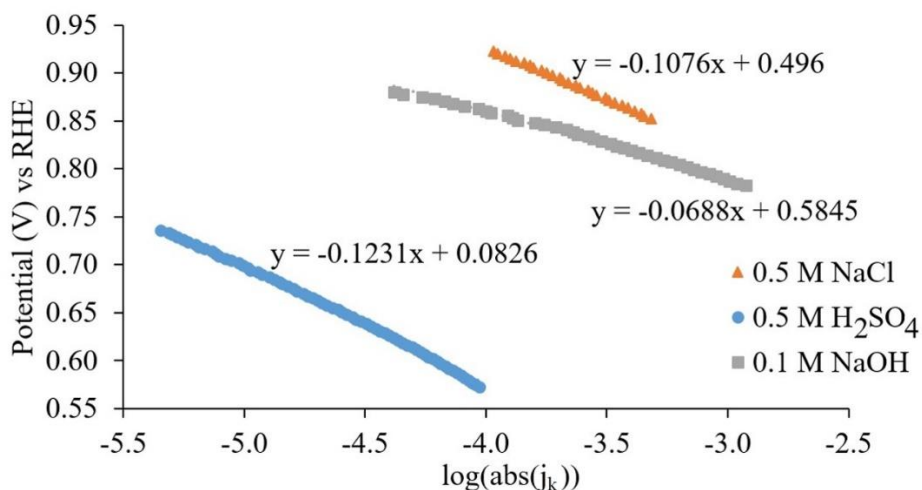


Figure 7. Tafel plots for the ORR on N-MCNT in 0.5 M NaCl solution.

No significant change in the onset potential of either of the studied materials is observed. Only a slight decrement in the current is observed, which may be attributed to detachment of the catalyst from the glassy carbon. The mass transfer limited current is unchanged, as the current seems to overlap at lower potential. The pattern of current increment in the mixed kinetic mass transfer region is similar before and after the stability test in 0.1 M NaOH solution. The high onset potential for the ORR and the slight decrease in the ORR activity make this catalyst suitable for seawater deoxygenation.

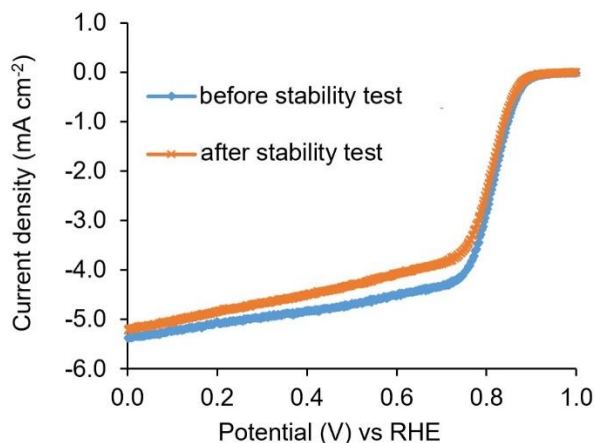


Figure 8. LSV before and after 1600 cycling (corresponding to 15 h of cycling) in 0.1 M NaOH for N-MCNTs.

4. CONCLUSIONS

- The graphite structure of CNTs is found to be unaffected by the process of nitrogen doping.
- Physical characterization was performed by XPS, XRD and HRTEM, and nanotubes were found to be unaffected by the doping process.
- The electrochemical studies indicate that N-MCNT is an active electrocatalyst for the ORR in 0.5 M NaCl. The onset potential for N-MCNT in 0.5 M NaCl (0.94 V vs RHE) is higher, compared to onset potential in alkaline (0.89 V vs RHE) and in acidic solutions (0.63 V vs RHE).
- The K-L plots suggest that the reaction on the studied catalyst follows a four-electron transfer pathway at lower potential.
- The dynamic stability test of 1600 CV cycles shows that N-MCNT is a stable and potential option as an ORR electrocatalyst in seawater deoxygenation.

ACKNOWLEDGEMENT

The authors are grateful to the Research Council of Norway for providing funding for URD for research abroad under the Industrial PhD scheme (Project no. 269533) and the Academy of Finland DEMEC project (Project no. 286266). The authors are grateful to Mr. Florian Speck, Helmholtz Institute Erlangen-Nürnberg, for ICP-MS analyses. The authors acknowledge the assistance from Mr. Wakshum Mekonnen Tucho, University of Stavanger, for HRTEM analyses.

References

1. U. R. Dotel, K. Vuorilehto, M. O. Sydnes, H. Urkedal, T. Hemmingsen, *Ind. Eng. Chem. Res.*, 55 (2016) 8235.
2. E. H. Yu, S. Cheng, K. Scott, B. Logan, *J. Power Sources*, 171 (2007) 275.
3. M. Lu, L. Guo, S. Kharkwal, H. Wu, H. Yong Ng, S. F. Yau Li, *J. Power Sources*, 221 (2013) 381.
4. U. R. Dotel, K. Vuorilehto, M. O. Sydnes, H. Urkedal, T. Hemmingsen, *Ind. Eng. Chem. Res.*, 56 (2017) 8954.
5. A. Sharma, V. Kumar, *J. Mater. Environ. Sci.*, 3 (2011) 76.
6. H. Yuan, Y. Hou, I. M. Abu-Reesh, J. Chen, Z. He, *Mater. Horiz.*, 3 (2016) 382.
7. H. A. Gasteiger, S. S. Kocha, B. Sompalli, F. T. Wagner, *Appl. Catal.*, B, 56 (2005) 9.
8. M. Shao, Q. Chang, J.-P. Dodelet, R. Chenitz, *Chem. Rev.*, 116 (2016) 3594.
9. Z. Wang, C. Cao, Y. Zheng, S. Chen, F. Zhao, *ChemElectroChem*, 1 (2014) 1813.
10. D. E. Grove, *Platinum Met. Rev.*, 1 (2003) 44.
11. V. A. Sethuram, J. W. Weidner, *Electrochim. Acta*, 20 (2010) 5683-5694.
12. C. Santoro, A. Stadlhofer, V. Hacker, G. Squadrito, U. Schröder, B. Li, *J. Power Sources*, 243 (2013) 499.
13. C. Santoro, A. Serov, C. W. N. Villarubia, S. Stariha, S. Babanova, K. Artyushkova, A. J. Schuler, P. Atanassov, *Sci. Rep.*, 5 (2015) 16596.
14. C. Santoro, A. Serov, L. Stariha, M. Kodali, J. Gordon, S. Babanova, O. Bretschger, K. Artyushkova, P. Atanassov, *Energy Environ. Sci.*, 9 (2016) 2346.
15. X. Ge, A. Sumboja, D. Wu, T. An, B. Li, F. W. T. Goh, T. S. A. Hor, Y. Zong, Z. Liu, *ACS Catal.*, 5 (2015) 4643.
16. X. Ma, S. Feng, S. Ji, *Int. J. Electrochem. Sci.*, 12 (2017) 7869.
17. L. Demarconnay, C. Coutanceau, J. M. Léger, *Electrochim. Acta*, 49 (2004) 4513.
18. B. B. Blizanac, P. N. Ross, N. M. Marković, *J. Phys. Chem. B*, 110 (2006) 4735.
19. B. B. Blizanac, P. N. Ross, N. M. Markovic, *Electrochim. Acta*, 52 (2007) 2264.
20. G. K. H. Wiberg, K. J. J. Mayrhofer, M. Arenz, *Fuel Cells*, 10 (2010) 575.
21. P. Singh, D. A. Buttry, *J. Phys. Chem. C*, 116 (2012) 10656.
22. A. Fazil, R. Chetty, *Electroanal.*, 26 (2014) 2380.
23. J. Perez, E. R. Gonzales, E. A. Ticianelli, *Electrochim. Acta*, 44 (1998) 1329.
24. J. S. Kim, E. Kuk, K. N. Yu, J. -H. Kim, S. J. Park, H. J. Lee, S. H. Kim, Y. K. Park, Y. H. Park, C.-Y. Hwang, Y. -K. Kim, Y. -S. Lee, D. H. Jeong, M. -H. Cho, *Nanomedicine*, 3 (2007) 95.
25. F. Davodi, M. Tavakkoli, J. Lahtinen, T. Kallio, *J. Catal.*, 353 (2017) 19.
26. P. H. Matter, E. Wang, M. Arias, E. J. Biddinger, U. S. Ozkan, *J. Phys. Chem. B*, 110 (2006) 18374.
27. Z. Chen, D. Higgins, H. Tao, R. S. Hsu, Z. Chen, *J. Phys. Chem. C*, 113 (2009) 21008.
28. Z. Chen, D. Higgins, A. Yu, L. Zhang, J. Zhang, *Energy Environ. Sci.*, 4 (2011) 3167.
29. E. N. Nxumalo, N. J. Coville, *Materials*, 3 (2010) 2141.
30. C. Dominguez, F. J. Perez-Alonso, K. L. G. de la Fuente, S. A. Al-Thabaiti, S. N. Basahel, A. O. Alyoubi, A. A. Alshehri, M. A. Pena, S. Rojas, *J. Power Sources*, 271 (2014) 87.
31. H. Zhang, H. Li, X. Li, B. Zhao, J. Yang, *Int. J. Hydrogen Energy*, 39 (2014) 16964.
32. M. Borghei, P. Kanninen, M. Lundahl, T. Susi, J. Sainio, I. Anoshkin, A. Nasibulin, T. Kallio, K. Tammeveski, E. Kauppinen, V. Ruiz, *Appl. Catal.*, B, 158 (2014) 233.
33. T. J. Schmidt, U. A. Paulus, H. A. Gasteiger, R. J. Behm, *J. Electroanal. Chem.* 508 (2001) 41.
34. S. R. K. Artyushkova, A. Serov, C. Santoro, I. Matanovic, P. Atanassov, *ACS Catal.*, 8 (2018) 3041.
35. L. Tammeveski, H. Erikson, A. Sarapuu, J. Kozlova, P. Ritslaid, V. Sammelselg, K. Tammeveski, *Electrochem. Commun.* 20 (2012) 15.
36. M. Jamnongwong, K. Loubiere, N. Dietrich, G. Hébrard, *Chem. Eng. J.*, 165 (2010) 758.

37. E. S. Beh, D. De Porcellinis, R. L. Gracia, K. T. Xia, R. G. Gordon, M. J. Aziz, *ACS Energy Lett.*, 2 (2017) 639.
38. N. Alexeyeva, K. Tammeveski, *Electrochem. Solid-State Lett.*, 10 (2007) F18.
39. J. Wang, M. Musameh, Y. Lin, *J. Am. Chem. Soc.*, 125 (2003) 2408.
40. Y. Cheng, Y. Tian, S. Tsang, C. Yan, *Electrochim. Acta*, 174 (2015) 919.

© 2019 The Authors. Published by ESG (www.electrochemsci.org). This article is an open access article distributed under the terms and conditions of the Creative Commons Attribution license (<http://creativecommons.org/licenses/by/4.0/>).